Energy Efficiency Analysis of LoRa Networks

Lam-Thanh Tu, Abbas Bradai, Yannis Pousset, Alexis I. Aravanis

Energy Efficiency Analysis of LoRa Networks

Lam-Thanh Tu, Abbas Bradai *Senior Member*, *IEEE*, Yannis Pousset and Alexis I. Aravanis

***Abstract*— In the present letter, a closed-form framework is derived for the system-level modelling, analysis and optimization of the energy efficiency (EE) in LoRa networks. The proposed framework is derived by exploiting stochastic geometry tools and associates the Long Range (LoRa) EE with the density of end-devices (EDs) and the ED transmit power. The analysis reveals the trends of the EE curve with respect to each of the two parameters while revealing the existence of an optimal transmit power that maximizes the EE. Thus, the proposed framework arises as a valuable tool, of significant practical value, for the optimization of the receiver/transmitter design, and of the network deployment in LoRa networks. The robustness of the framework is verified even at the asymptotic cases of fully-loaded or sparsely-loaded LoRa networks.**

***Index Terms*— LoRa, LPWAN, LoRaWAN, Energy Efficiency, Stochastic Geometry, System-Level Analysis.**

I. Introduction

The advent of the Internet of Things (IoT) and the exponential increase of IoT devices, has shaped, to a great extent, the emerging 5G networks through the development of relevant 5G services, such as the massive machine-type communications (MTC). IoT devices are also expected to play an instrumental role beyond 5G, spearheading the development of 6G networks. Particularly, as opposed to the local connections in 5G, IoT devices in 6G are expected to be connected, over large networks, under holistic "smart city" frameworks [1]. In this course, the development of long range, low power wide area networks (LPWAN) is of paramount importance, in order to support energy efficient and scalable IoT networks of wide coverage [2]–[4].

One of the key technologies ushering IoT networks and particularly LPWAN into this new era is the Long Range (LoRa) patented technology. LoRa is employed for delivering power-efficient, long-distant transmissions in LPWAN [3]. LoRa can be applied to a wide range of IoT devices and applications that belong to different quality-of-service (QoS) tiers. Such applications include smart buildings, smart cities, smart agriculture, and smart metering of critical infrastructure such as water reserves [3]. LoRa can support this wide variety of applications through the appropriate adjustment of its intrinsic parameters, such as the spreading factor (SF), the coding rate (CR) and the bandwidth (BW). To exploit this flexibility and devise relevant optimization strategies, for the network deployment and receiver/transmitter design, the system-level analysis of LoRa networks is imperative.

In this direction, stochastic geometry (SG) tools and the theory of spatial point process has been employed for modelling random deployments of end-devices (EDs) in LoRa networks, toward providing tractable network models amenable to optimization. Such SG performance analyses of LoRa networks were provided in [5], [6]. In particular, the authors of [5] employ the SG introduced metric of coverage probability (Pcov) (i.e. the complementary cumulative distribution function (CDF) of the signal-to-interference-plus-noise ratio (SINR)) for the analysis of LoRa networks, assuming however, for the sake of simplicity, that the spatial correlations between the signal-to-noise ratio (SNR) and the signal-to-interference ratio (SIR) at the gateway are independent. Building upon this framework, a novel, closed-form expression of the Pcov was introduced in [6] taking into account the correlation between the SNR and SIR at the gateway. This work however, focuses on the spectral efficiency (SE) aspects of the system rather than the energy efficiency (EE) aspects, that are examined herein. The Pcov has also been employed to examine EE network aspects, like in the case of [7] where the authors focus on the EE aspects of heterogeneous cellular networks (HetNets). However, such HetNets are fundamentally different from LoRa networks. As a result, the differences in protocols and radio interfaces give rise to fundamentally different mathematical frameworks and analyses, than the one examined herein.

Overcoming these above-mentioned limitations, the present paper provides a holistic framework for the system-level performance analysis of LoRa networks with respect to the EE. In particular, the system-level EE of LoRa networks is computed, herein, by a closed-form expression, for the first time in the literature (to the best of the author's knowledge), while the accuracy of the framework is validated by relevant simulations. More importantly, the derived expressions associate the overall network EE to fundamental network and ED design parameters, allowing for the optimal receiver design and the optimization of the LoRa network parameters, with respect to the maximization of the network EE.

II. System Model

A. LoRa Network Modeling

Let us consider an uplink LoRa network comprising a single gateway located at the centre of a disc of radius R. A set of EDs is overlaid within the disc, following a homogeneous Poisson point process (PPP) of density $\lambda = \overline{N}/\mathcal{Y}$. $\overline{N}$ is the average number of EDs and $\mathcal{Y} = \pi R^2$ is the area of the disc, which is divided into six non-overlapping regions. These six regions are defined by 6 concentric cycles, giving rise to a central disc region and five regions at the outer rings. Each region is assigned a unique SF denoted by $k \in \{7, \ldots, 12\}$. The SF of each region increases monotonically with the distance from the gateway. Hence, the closer to the gateway,

Manuscript received xxx, 2021; revised Mar. 12, 2021; accepted May 23, 2021. Date of publication xxx, 2021; date of current version xxx, 2021. This work was supported in part by the CPER/FEDER project "Intelligent Networks II" under grant agreement NUMERI06 and the European Commission through the PathFinder project under grant agreement 891030. The associate editor coordinating the review of this article and approving it for publication was J. Lee. (*Corresponding author: Lam-Thanh TU*)

L.-T. Tu, A. Bradai and Y. Pousset are with the Institute XLIM, University of Poitiers, 86000 Poitiers, France (email: lam.thanh.tu@univ-poitiers.fr; abbas.bradai@univ-poitiers.fr; yannis.pousset@univ-poitiers.fr).

Alexis I. Aravanis is with Université Paris-Saclay, CNRS, CentraleSupélec, L2S , 91192 Gif-sur-Yvette, France. (alexis.aravanis@centralesupelec.fr).

TABLE I: LoRa characteristics [5]

SF, k	γ_{D} [dBm]	Range
7	-6	0 - $R/6$
8	-9	$R/6$ - $R/3$
9	-12	$R/3$ - $R/2$
10	-15	$R/2$ - $2R/3$
11	-17.5	$2R/3$ - $5R/6$
12	-20	$5R/6$ - R

the smaller the SF, as depicted in Table I. Signals with different SFs are perfectly orthogonal [5]; thus, the interference created by EDs of SF $\widetilde{k}$, $\widetilde{k} \neq k \in \{7,\ldots,12\}$, is cancelled at the gateway. The interference from different technologies that may operate at the same frequencies is also not considered, as is typically the case in the literature [5].

B. Channel Modelling

The packets sent by the EDs to the gateway are subjected to large-scale path-loss and small-scale fading. The impact of the shadowing is not taken into account, as its effects can be simply incorporated into the analysis by appropriately scaling the value of λ [8].

1) Small-scale fading: Let us denote by h_e the small-scale fading from an arbitrary ED e to the gateway. Assuming h_e follows a Nakagami-m distribution of shape and spread parameters, m_e and Ω_e, respectively, then the channel gain h_e^2 follows a Gamma distribution of shape and scale parameters, m_e and $\theta_e = m_e/\Omega_e$, respectively.

2) Large-scale path-loss: Considering a transmission link from an arbitrary ED e to the gateway, the large-scale path-loss is given by

$$L_e = l\left(r_e\right) = K_0 r_e^{\beta}, \tag{1}$$

where $\beta > 2$ is the path-loss exponent and r_e is the distance from ED e to the gateway; $K_0 = \left(4\pi f_c/c\right)^2$ is the path-loss constant, with f_c being the carrier frequency and c the speed of light.

C. ED Power Consumption Modelling

The power consumption of an arbitrary ED of SF k can be modelled by taking into account the different operational states of the ED. In particular, an ED can be in one of 11 different states denoted by $S_{i,k}$, $i \in \{1,\ldots,11\}, k \in \{7,\ldots,12\}$ [9], as shown in Table II. In Table II, the duration of each state i of an ED of SF k, is denoted by $T_{S_{i,k}}$, $i \in \{1,\ldots,11\}$, $k \in \{7,\ldots,12\}$, and only the duration of the states S_3, S_5 and S_{11} depends on the SF of the ED, i.e., $T_{S_{i,k}} = T_{S_i}, \forall k, i \in \{1,\ldots,11\} \setminus \{3,5,11\}$. For the SF dependent states, $T_{S_{3,k}}$ refers to the time on air (ToA) of the transmitted packet and is given by [9]:

$$T_{S_{3,k}} = T_{\mathrm{sym},k} N_{\mathrm{pac},k} \tag{2}$$

$$N_{\mathrm{pac},k} = \left(N_{\mathrm{pre}} + 4.25\right) + 8 \tag{3}$$
$$+ \max\left\{\left\lceil \frac{8PL - 4k + 28 + 16CRC - 20H}{4\left(k - 2DE\right)} \right\rceil \left(4 + \mathrm{Cr}\right), 0\right\},$$

where $T_{\mathrm{sym},k} = 2^k/\mathrm{Bw}$ is the time to transmit one symbol under SF k, Bw is the transmission bandwidth, and $N_{\mathrm{pac},k}$ is the packet length of SF k (in symbols). N_{pre} is the number of preamble symbols, PL is the physical payload length (in bytes), and CRC indicates the presence (i.e. $CRC = 1$) or absence (i.e. $CRC = 0$) of a cyclic redundancy check (CRC) field. $H = 0$, indicates that the header is enabled and $H = 1$ that it isn't. For EDs residing in the close proximity of the gateway, i.e. for $k = \{7,\ldots,10\}$, then $DE = 0$, whereas for EDs in distant regions, i.e. for $k = \{11, 12\}$, $DE = 1$, indicating in the latter case that the low data rate optimization is enabled. $\mathrm{Cr} \in \{1,\ldots,4\}$ is the coding rate and $\lceil\cdot\rceil$ and $\max$ are the ceiling and maximum functions respectively. Last but not least, the duration of the sleep state, denoted by $T_{S_{11,k}}$, is

TABLE II: States and current consumption of an ED; with supplied voltage, V = 3.3 volt, [9].

States S_i	Description	Duration T_{S_i} [ms]	Current [mA] consumption I_{S_i}
1	wake up	168.2	22.1
2	radio preparation	83.8	13.3
3	transmission	Eq. (2)	I_{tx}
4	wait 1st window	983.3	27
5	1st receive window	[9, Table 6]	38.1
6	wait 2nd window	[9, Eq. 4]	27.1
7	2nd receive window	33.0	35.0
8	radio off	147.4	13.2
9	post processing	268.0	21.0
10	turn off sequence	38.6	13.3
11	sleep	Eq. (4)	45 $\times 10^{-3}$

$$T_{S_{11,k}} = T_{\mathrm{tot},k} - \sum\nolimits_{i=1}^{10} T_{S_{i,k}}, \tag{4}$$

where $T_{\mathrm{tot},k} = \max\left\{T_{\mathrm{in}}, \left(1/\rho\right) T_{S_{3,k}}\right\}$ is the total time for one transmission. $T_{\mathrm{tot},k}$ is defined as the maximum between the highest permitted ToA in LoRa networks and the inter-arrival time between two messages, denoted by T_{in}. $\rho \in (0,1]$ is the duty cycle.

III. System-level Energy Efficiency performance

The system-level EE (measured in bits/Joule) refers to the number of bits successfully transmitted per unit energy over the whole network. Mathematically, the system-level EE is formulated as follows [7]:

$$\mathrm{EE} = \frac{\sum_{k=7}^{12} \rho \lambda_k k N_{\mathrm{pac},k} P_{\mathrm{suc}_k}\left(\gamma_{\mathrm{D},k}\right)}{\sum_{k=7}^{12} \rho \lambda_k \left(T_{S_{3,k}} P_{\mathrm{tx}} + E_{\mathrm{cir},k}\right) + \left(1-\rho\right)\lambda_k E_{\mathrm{sl},k}}, \tag{5}$$

where λ_k is the density of EDs of SF k and since the considered PPP is homogeneous, λ_k is the same in all regions, i.e., $\lambda_k = \lambda, \forall k$. $P_{\mathrm{tx}} = V I_{\mathrm{tx}}$ is the transmit power of the EDs. $E_{\mathrm{cir},k} = \sum_{i=1, i\neq 3}^{10} T_{S_{i,k}} V I_{S_{i,k}}$ is the energy consumption of an ED of SF k, for all states apart from the transmission and sleep states. $E_{\mathrm{sl},k} = T_{S_{11,k}} V I_{S_{11,k}}$ is then the energy consumption of an ED of SF k in the sleep state. V is the supplied voltage and $I_{S_{i,k}} = I_{S_i}$ is the current consumption at state i and is independent of the SF k. In the transmission state the current consumption is denoted by $I_{S_3} = I_{\mathrm{tx}}$, for simplicity in the notation, as also defined in Table II. $P_{\mathrm{suc}_k}\left(\gamma_{\mathrm{D},k}\right)$ is the probability of a successful transmission for an ED of SF k and is defined by the joint probability [7]

$$P_{\mathrm{suc}_k}\left(\gamma_{\mathrm{D},k}\right) = \Pr\left\{\mathrm{SIR}_k \geq \gamma_{\mathrm{I}}, \mathrm{SNR}_k \geq \gamma_{\mathrm{D},k}\right\}, \tag{6}$$

where $\Pr\{\cdot\}$ is the probability operator; γ_{I} is the rejection threshold, which does not depend on the SF, k, due to the lack of inter-region interference across regions of different SFs k [4] (i.e. only intra-region interference is considered). $\gamma_{\mathrm{D},k}$ is the QoS threshold which depends on the SF k [6] and is given in Table I. The SIR and the SNR of EDs with SF k are denoted by, $\mathrm{SIR}_k = S_k/I_{S_k}$, and $\mathrm{SNR}_k = S_k/\sigma^2$ respectively, where $S_k = P_{\mathrm{tx}} h_{0,k}^2 / L_{0,k}$ is the signal received at the gateway from the ED of interest and $I_{S_k} = P_{\mathrm{tx}} \sum_{i \in \Psi^{\mathrm{A}_k} \setminus (0)} \left(h_{i,k}^2 / L_{i,k}\right)$ is

the aggregate interference created at the gateway, by all active EDs of SF k apart from the ED of interest; $\Psi^{\mathrm{A}_k\backslash(0)}$ is the set of active EDs of SF k apart from the ED of interest; $h^2_{0,k}$, $h^2_{i,k}$, $L_{0,k}$ and $L_{i,k}$ are the small-scale fading and large-scale path-loss, respectively, from the ED of interest and from the interfering ED i of SF k; $\sigma^2 = -174 + \mathrm{NF} + 10\log_{10}\mathrm{Bw}$ (dBm) is the additive white Gaussian noise (AWGN) noise variance; NF and log are the noise figure and the logarithm function.

In LoRa, the number of concurrent transmissions is limited due to the strict constraint of the duty cycle [5]. As a consequence, it is commonly assumed that the strongest interfering signal will dominate the aggregate interference [5], [6]. Moreover, as proved in [6], the exact closed-form expression of the P_{suc} cannot be obtained based on the instantaneous small-scale fading. Hence, the average small-scale fading can be employed instead, and due to the aforementioned assumption the interference created only by the dominant interferer can be considered, to derive the following approximation of P_{suc}: $\widetilde{P_{\mathrm{suc}k}}(\gamma_{\mathrm{D},k}) = \Pr\left\{\widetilde{\mathrm{SIR}}_k \geq \gamma_{\mathrm{I}}, \widetilde{\mathrm{SNR}}_k \geq \gamma_{\mathrm{D},k}\right\}$, where $\widetilde{\mathrm{SIR}}_k = \left(P_{\mathrm{tx}}\mathbb{E}\left\{h^2_{0,k}\right\}/L_{0,k}\right) / \left(\max_{i\in\Psi^{\mathrm{A}_k\backslash(0)}} P_{\mathrm{tx}}\mathbb{E}\left\{h^2_{i,k}\right\}/L_{i,k}\right)$, $\widetilde{\mathrm{SNR}}_k = P_{\mathrm{tx}}\mathbb{E}\left\{h^2_{0,k}\right\}/\left(L_{0,k}\sigma^2\right)$, and $\mathbb{E}\{\cdot\}$ is the mean operator. $\widetilde{P_{\mathrm{suc}k}}(\gamma_{\mathrm{D},k})$ is then calculated in Theorem 1.

Theorem 1: Let us define the notations: $\delta = 2/\beta$, $\mathcal{A}_k = \pi\lambda^A_k\left(R^2_{out,k} - R^2_{in,k}\right), \mathcal{B}_k = \left(R^2_{out,k} - R^2_{in,k}\right)^{-1}, \mathcal{C} = \left(\mathcal{F}\gamma_{\mathrm{I}}/K_0\right)^{\delta}$, $\mathcal{D}_k = \left(\gamma_{\mathrm{D},k}\sigma^2\right)/P_{\mathrm{tx}}$, $\mathcal{Q}_{in,k} = \mathcal{F}\left(R^{\beta}_{in,k}K_0\right)^{-1}, \mathcal{Q}_{out,k} = \mathcal{F}\left(R^{\beta}_{out,k}K_0\right)^{-1}$, $\mathcal{F} = m\theta$, where $R_{in,k}$ and $R_{out,k}$ are the inner and outer radius of the region with SF k, respectively; $\lambda^A_k = \rho\lambda_k$ is the active density of SF k. The approximated probability of successful transmission for an ED of SF k is then computed as follows:

$$\widetilde{P_{\mathrm{suc}k}}(\gamma_{\mathrm{D},k}) = c_{3,k}\left[\upsilon_{1,k}\left(\mathcal{V}_1\left(\mathcal{Q}_{in,k}\right) - \mathcal{V}_1\left(c_{1,k}\right)\right) \times \left(\mathcal{A}_k\mathcal{B}_k\mathcal{C}\right)^{-1} + \exp\left(-\mathcal{A}_k\right)\upsilon_{4,k}\right], \quad (7)$$

where $\exp(\cdot)$ and $\min(\cdot)$ are the exponential and the minimum function; $\mathbf{1}(x)$ is the indicator function which is equal to 1 if $x > 0$ and 0 otherwise; $c_{1,k} = \max\{\gamma_I\mathcal{Q}_{out,k}, \mathcal{D}_k\}$, $c_{2,k} = \max\{\mathcal{Q}_{out,k}, \mathcal{D}_k\}$, $c_{3,k} = \mathcal{B}_k(\mathcal{F}/K_0)^{\delta}$, $\upsilon_{4,k} = \upsilon_{1,k}\upsilon_{2,k} + \upsilon_{3,k}$, $\upsilon_{1,k} = \mathbf{1}(\mathcal{Q}_{in,k} - c_{1,k})$, $\upsilon_{2,k} = \left((c_{2,k})^{-\delta} - (\gamma_I\mathcal{Q}_{out,k})^{-\delta}\right)\mathbf{1}(\gamma_I\mathcal{Q}_{out,k} - c_{2,k})$, $\upsilon_{3,k} = \left((c_{2,k})^{-\delta} - (\mathcal{Q}_{in,k})^{-\delta}\right)\mathbf{1}(\gamma_I\mathcal{Q}_{out,k} - \mathcal{Q}_{in,k})\,\mathbf{1}(\mathcal{Q}_{in,k} - \mathcal{D}_k)$, $\mathcal{V}_{1,k}(x) = \exp(-\mathcal{A}_k u_1(x))$, and $u_{1,k}(x) = \mathcal{BC}(x)^{-\delta} + 1 - \mathcal{B}R^2_{out,k}$.

Proof: See Appendix I. □

It should be noted that as opposed to P_{suc_k} that cannot be defined, $\widetilde{P_{\mathrm{suc}k}}$ can be derived in closed-form. This allows for the formulation of a rigorous mathematical framework that allows for the study of the trends of the EE with respect to key network parameters such as λ_k and P_{tx}. Moreover, the $\widetilde{P_{\mathrm{suc}k}}(\gamma_{\mathrm{D},k})$ of Theorem 1 can be computed in closed-form even if the inter-region interference across regions of different SFs is taken into account, provided that SIRs of all regions and SFs are independent to each other.

IV. Performance Trends

The derived framework is hereafter employed to gain insights into the performance trends of the EE under the impact of two essential system parameters, i.e., the transmit power P_{tx} and the density of EDs λ. For simplicity in the notation the EE and the $\widetilde{P_{\mathrm{suc}k}}$ are denoted by $\mathrm{EE} = \mathcal{E}(\varpi)$ and $\widetilde{P_{\mathrm{suc}k}} = \mathcal{P}_k(\varpi)$ where ϖ denotes the system parameter that is under consideration each time. The impact of the two system parameters, i.e., of $\varpi = \lambda$ and of $\varpi = P_{\mathrm{tx}}$, is examined by the following two propositions, respectively.

Proposition 1: Let us denote $\lambda = \varpi$, $\mathcal{E}(\varpi)$ is a convex, monotonic decreasing function with respect to ϖ. When $\varpi \to 0$, the asymptotic formulation of $\mathcal{E}(\varpi)$ is given by $\mathcal{E}(\varpi) \overset{\varpi\to 0}{=} \phi^{-1}\sum_{k=7}^{12}\rho k N_{\mathrm{pac},k}c_{3,k}\left(\upsilon_{4,k} + \upsilon_{5,k}\right)$ where $\upsilon_{5,k} = \left(\left(\max\{\mathcal{D}_k, \gamma_I\mathcal{Q}_{out,k}\}\right)^{-\delta} - \left(\mathcal{Q}_{in,k}\right)^{-\delta}\right) \times\mathbf{1}\left(\mathcal{Q}_{in,k} - \max\{\gamma_I\mathcal{Q}_{out,k}, \mathcal{D}_k\}\right)$ and $\phi = \sum_{k=7}^{12}\rho\left(T_{S_{3,k}}P_{\mathrm{tx}} + E_{\mathrm{cir},k}\right) + (1-\rho)E_{\mathrm{sl},k}$.

Proof: See Appendix II. □

Remark 1: Proposition 1 proves that network densification significantly decreases the EE. This effect is antipodal to the effect of densification (i.e. of the increase of $\overline{N}$) to the spectral efficiency [6]. Moreover, the asymptotic formulation of $\mathcal{E}(\varpi)$ of Proposition 1 is further simplified if $P_{\mathrm{tx}} \gg 1$, and the EE is then given by $\mathcal{E}(\varpi) = \phi^{-1}\sum_{k=7}^{12}\rho k N_{\mathrm{pac},k}c_{3,k}$.

Proposition 2: Let us denote $P_{\mathrm{tx}} = \varpi$. $\mathcal{E}(\varpi)$ is then a pseudo-concave function, that can be maximized by the global optimum denoted by $\varpi^* = P^*_{\mathrm{tx}}$.

Proof: See Appendix III. □

Remark 2: Proposition 2 evinces that there always exists a global optimum, i.e., P^*_{tx} that maximizing the EE. This allows for optimally configuring the network and the receiver design to maximize the EE, by optimizing parameters such as the ED current consumption; as is demonstrated below.

V. Numerical Results

In the present section, numerical results are provided to verify the accuracy of the proposed mathematical framework and to substantiate the findings presented in Section IV. In this direction, a class of IoT devices is considered, (a class of payment terminals), characterized by certain transmission parameters that are concretely defined for the framework of machine to machine (M2M) communications [10]. Unless otherwise stated, the network and ED parameters are the following: $\beta = 3.5$, Bw = 125 kHz, NF = 6 dBm, γ_{I} = 1 dBm, f_c = 868 MHz, R = 6000 m, $m = \Omega = 3.5$, $H = 0$, $N_{\mathrm{pre}} = 8$, $CRC = 1$; $\overline{N}$ = 2000, PL = 24 bytes, Cr = 4/5, I_{tx} = 80 mA, V = 3.3 volt, and T_{in} = 120 seconds.

Fig. 1 presents the system-level EE versus the average number of EDs $\overline{N}$ for (a) different fading channels, i.e., Rayleigh (of $m = \Omega = 1$) and no fading ($m = \Omega = 20$), and (b) for different payload sizes. We observe that the proposed framework denoted by "Frame" practically coincides with the Monte Carlo simulations that account only for the dominant interferer and the average small-scale fading denoted by "Max"; and that the proposed approximation is also tight to the exact Monte Carlo simulations considering aggregate interference and instantaneous small-scale fading denoted by

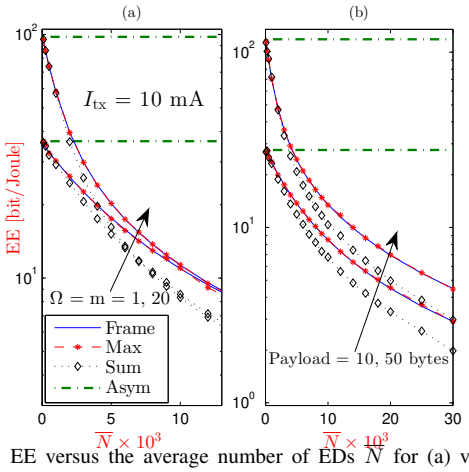

Fig. 1. EE versus the average number of EDs $\overline{N}$ for (a) various fading distributions and (b) various payload sizes.

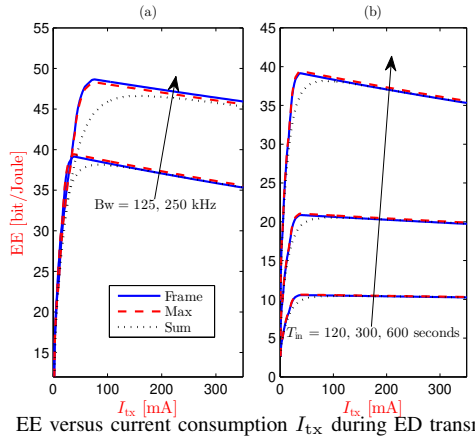

Fig. 2. EE versus current consumption $I_{\rm tx}$ during ED transmission for (a) different values of BW and (b) different inter-arrival times $T_{\rm in}$.

"Sum". Moreover, the figure verifies the conclusion arising from Proposition 1 that the network EE decreases with $\overline{N}$. The robustness of the analysis is also highlighted by the fact that when $\overline{N}$ tends to zero, the EE tends to the obtained asymptotic result denoted by "Asym" and not to infinity. In Fig. 1(a), it is evident that when no fading is considered the network EE is higher than in the presence of Rayleigh fading. However, as $\overline{N}$ increases, and the network transitions from a noise-limited to an interference-limited regime, both lines converge to the same point. That is since the network transitions from a regime where the fading effect on the channel gain is pronounced, to a regime where it is not. Fig. 1(b) illustrates the impact of the payload size on the network EE. Higher payload sizes allow for a higher EE, particularly at the noise-limited regime (i.e. for small $\overline{N}$). However, since a bigger payload size entails a longer ToA, as $\overline{N}$ and implicitly as the interference increases, this affects the bigger payload sizes more and their EE converges to the EE of smaller payload sizes.

Fig. 2 depicts the network EE with respect to the current consumption $I_{\rm tx}$ under (a) different BW values and (b) different inter-arrival times between two transmissions, $T_{\rm in}$. Again the tightness of the approximation "Frame" is verified, with respect to both approximate "Max" and exact Monte Carlo simulations "Sum". More importantly, figure 2 verifies the finding of Proposition 2 that there always exists a global optimum of $I_{\rm tx}$ (or $P_{\rm tx}$) for which the EE reaches its peak. Fig. 2(a) illustrates also the effect of BW onto the LoRa EE. In particular, doubling the BW improves the EE by approximately 10 bits/Joule for only a minimal increase of $I_{\rm tx}$. Fig. 2(b) demonstrates that increasing $T_{\rm in}$ also improves substantially the EE, since the SIR increases when $T_{\rm in}$ increases. That is since, when $T_{\rm in}$ increases, more EDs are in sleep mode, hence, less interference is created.

VI. Conclusion

The derived, closed-form framework, fully characterizes the system EE regarding the transmit power and the density of EDs in LoRa networks, even in the asymptotic cases. The proposed scheme is considered as a valuable tool for optimizing receiver design and network deployment in IoT LoRa networks, of significant practical value.

Appendix I
Proof of Theorem 1

In this section, the approximated probability of successful transmission $\widetilde{P_{{\rm suc}k}}\left(\gamma_{{\rm D},k}\right)$ of an ED of SF k, is derived. Let us commence with the CDF and implicitly with the the probability density function (PDF) of the approximated intended signal and of the interference. These CDFs are given by:

$$F_{S_k}\left(x\right)=\Pr\left\{\mathcal{F}/\left(K_0 r_{0,k}^{\beta}\right)\leq x\right\}\overset{(a)}{=}\mathbf{1}\left(R_{out,k}-\left(\left(xK_0\right)\right)^{-1/\beta}\right.$$
$$\left.\times\mathcal{F}^{1/\beta}\right)\left[2\mathcal{B}_k\int_{r=\max\left\{R_{in,k},\left(\mathcal{F}/\left(xK_0\right)\right)^{1/\beta}\right\}}^{R_{out,k}} rdr\right]=\mathbf{1}\left(x-\mathcal{Q}_{in,k}\right)$$
$$+\mathcal{B}_k\left[R_{out,k}^2-\left(\mathcal{F}/\left(xK_0\right)\right)^{\delta}\right]\mathbf{1}\left(x-\mathcal{Q}_{out,k}\right)\mathbf{1}\left(\mathcal{Q}_{in,k}-x\right),$$
$$f_{S_k}\left(x\right)=dF_{S_k}\left(x\right)/dx=\delta\mathcal{B}_k\mathcal{F}^{\delta}\left(K_0\right)^{-\delta}x^{-\delta-1}$$
$$\times\mathbf{1}\left(x-\mathcal{Q}_{out,k}\right)\mathbf{1}\left(\mathcal{Q}_{in,k}-x\right),$$
$$F_{I_{S_k}}\left(x\right)=\Pr\left(\max_{i\in\Psi^{A_k}\setminus(0)}\left\{\mathcal{F}/\left(K_0 r_{i,k}^{\beta}\right)\right\}<x\middle|\, i\right)$$
$$\overset{(b)}{=}\sum\nolimits_{o=0}^{\infty}\left(F_{I_{S_{i,k}}}\left(x\right)\right)^{o}\left(\exp\left(-\mathcal{A}_k\right)\left(\mathcal{A}_k\right)^{o}\right)/\left(o!\right)$$
$$\overset{(c)}{=}\exp\left(-\mathcal{A}_k\left(1-\mathcal{B}_k\left[R_{out,k}^2-\left(\mathcal{F}\right)^{\delta}\left(xK_0\right)^{-\delta}\right]\right.\right.$$
$$\left.\left.\times\mathbf{1}\left(x-\mathcal{Q}_{out,k}\right)\mathbf{1}\left(\mathcal{Q}_{in,k}-x\right)-\mathbf{1}\left(x-\mathcal{Q}_{in,k}\right)\right)\right), \tag{8}$$

where $\mathcal{A}_k$, $\mathcal{B}_k$, $\mathcal{F}$ are given in Theorem 1; (a) is attained by inputting the PDF of the distance r, i.e. $f_r(x)=2x\mathcal{B}_k$ and by applying the constraint $R_{in,k}\leq r_{0,k}<R_{out,k}$; (b) employs the order statistic for computing the CDF of the max of o iid random variables (RVs), while averaging over all possible values of o by employing the probability mass function (PMF) of Poisson distribution with mean $\mathcal{A}_k$; and (c) is attained by using the definition of exponential function $\exp\left(x\right)=\sum_{i=0}^{\infty}x^i/i!$. Having obtained the PDF and CDF of S_k and I_{S_k}, $\widetilde{P_{{\rm suc}k}}\left(\gamma_{{\rm D},k}\right)$ is then computed as

$$\widetilde{P_{{\rm suc}k}}\left(\gamma_{{\rm D},k}\right)=\Pr\left\{\widetilde{\rm SIR}_k\geq\gamma_{\rm I},\widetilde{\rm SNR}_k\geq\gamma_{{\rm D},k}\right\}$$
$$\overset{(a)}{=}\mathcal{B}_k\delta\mathcal{F}^{\delta}\left(K_0\right)^{-\delta}\int_{x=\mathcal{D}_k}^{\infty}x^{-\delta-1}\mathbf{1}\left(x-\mathcal{Q}_{out,k}\right)\mathbf{1}\left(\mathcal{Q}_{in,k}-x\right)$$
$$\times\exp\left(-\mathcal{A}_k\left(1-\mathcal{B}_k\left[R_{out,k}^2-x^{-\delta}\left(\mathcal{F}\gamma_{\rm I}/K_0\right)^{\delta}\right]\right.\right.$$
$$\left.\left.\times\mathbf{1}\left(x-\gamma_{\rm I}\mathcal{Q}_{out,k}\right)\mathbf{1}\left(\gamma_{\rm I}\mathcal{Q}_{in,k}-x\right)-\mathbf{1}\left(x-\gamma_{\rm I}\mathcal{Q}_{out,k}\right)\right)\right)dx,$$
$$=\delta\mathcal{B}_k\mathcal{F}^{\delta}\left(K_0\right)^{-\delta}\left(J_1+J_2\right)\mathbf{1}\left(\mathcal{Q}_{in,k}-\mathcal{D}_k\right), \tag{9}$$

where $\mathcal{D}_k$ are given in Theorem 1; we obtain (a) by inputting $f_{S_k}\left(x\right)$ and $F_{I_{S_k}}\left(x\right)$ into (8); J_1 and J_2 are given by:

$$J_2=\left(\exp\left(-\mathcal{A}_k\right)\int_{x=\max\left\{\mathcal{D}_k,\mathcal{Q}_{out,k}\right\}}^{\mathcal{Q}_{in,k}}x^{-\delta-1}dx\right)\mathbf{1}\left(\gamma_{\rm I}\mathcal{Q}_{out,k}-\mathcal{Q}_{in,k}\right)$$

$$J_1 = \Bigg(\int_{x=\max\{\mathcal{D}_k, Q_{out,k}\}}^{Q_{in,k}} x^{-\delta-1} \exp\Big(-\mathcal{A}_k \Big(1 - \mathcal{B}_k \Big[R_{out,k}^2 - \mathcal{C} x^{-\delta}\Big] \times \mathbf{1}\left(x - \gamma_{\mathrm{I}} Q_{out,k}\right)\Big)\Big) dx \Bigg) \mathbf{1}\left(Q_{in,k} - \gamma_{\mathrm{I}} Q_{out,k}\right). \quad (10)$$

The integrations J_1 and J_2 in (10) are evaluated by using the following: i) given $0 < a < b < +\infty$ and $0 < c < 1$, we have $\int_{x=a}^{b} (x)^{-c-1} dx = c^{-1}\left((a)^{-c} - (b)^{-c}\right)$; ii) given $0 < a < b < +\infty$, $0 < c < 1$ and $0 < d < +\infty$, we have $\int_{x=a}^{b} x^{-c-1} \exp\left(-dx^{-c}\right) dx = (cd)^{-1}\left(\exp\left(-db^{-c}\right) - \exp\left(-da^{-c}\right)\right)$. Finally, substituting J_1 and J_2 into (9), concludes the proof.

Appendix II
Proof of Proposition 1

The behaviour of the EE with respect to the density of EDs is studied in this section. The EE is given by:

$$\mathcal{E}(\varpi) = \frac{\sum_{k=7}^{12} \rho \lambda_k k N_{\mathrm{pac},k} \widetilde{P_{\mathrm{suc}\,k}}\left(\gamma_{\mathrm{D},k}, \lambda_k\right)}{\sum_{k=7}^{12} \rho \lambda_k \left(T_{S_{3,k}} P_{\mathrm{tx}} + E_{\mathrm{cir},k}\right) + (1-\rho)\lambda_k E_{\mathrm{sl},k}} \overset{(a)}{=} \phi^{-1} \sum_{k=7}^{12} \rho k N_{\mathrm{pac},k} \mathcal{P}_k(\varpi), \quad (11)$$

where ϕ is defined in Proposition 1, (a) holds due to the homogeneity of the PPP, i.e., $\lambda_k = \lambda, \forall k$. Hence, the $\mathcal{P}_k(\varpi)$ is identical for all k, and for simplicity the subscript k can be omitted. Moreover, from (11), it becomes evident that the behaviour of $\mathcal{E}(\lambda = \varpi)$ is defined only by the behaviour of $\mathcal{P}_k(\varpi) = \mathcal{P}(\varpi)$. Hence, studying the trends of $\mathcal{P}(\varpi)$ suffices. The first-order derivative of $\mathcal{P}(\varpi)$ is:

$$\dot{\mathcal{P}}(\varpi) = \frac{\pi\rho}{\mathcal{B}} c_3 \left[\frac{L_1(\varpi)\upsilon_1}{(\mathcal{A}(\varpi))^2 \mathcal{BC}} - \exp\left(-\mathcal{A}(\varpi)\right)\upsilon_4\right] < 0$$
$$L_1(\varpi) = \mathcal{A}(\varpi)\left(u_1(c_1)\mathcal{V}_1(\varpi; c_1) - u_1(\mathcal{Q}_{in})\mathcal{V}_1(\varpi; \mathcal{Q}_{in})\right)$$
$$- \left(\mathcal{V}_1(\varpi; \mathcal{Q}_{in}) - \mathcal{V}_1(\varpi; c_1)\right) = \left(1 + \mathcal{A}(\varpi) u_1(c_1)\right)$$
$$\times \mathcal{V}_1(\varpi; c_1) - \left(1 + \mathcal{A}(\varpi) u_1(Q_{in})\right)\mathcal{V}_1(\varpi; \mathcal{Q}_{in}) < 0, \quad (12)$$

where $\dot{f}(x) = df(x)/dx$ is the first-order derivative of f with respect to x. (12) holds due to the fact that $\left(1 + \mathcal{A}(\varpi) u_1(x)\right)\mathcal{V}_1(\varpi; x)$ is a monotonically decreasing function of x and to the fact that $c_1 > Q_{in}$. From (11) and (12), it holds that the EE, monotonically decreases with λ. The convexity of the EE is proven by taking the first-order derivative of $\dot{\mathcal{P}}(\varpi)$, defined in (12), with respect to ϖ:

$$\ddot{\mathcal{P}}_k(\varpi) = c_4 \left[\frac{L_2(\varpi)\upsilon_1}{(\mathcal{A}(\varpi))^3 \mathcal{BC}} + \exp\left(-\mathcal{A}(\varpi)\right)\upsilon_4\right] > 0$$
$$L_2(\varpi) = (\mathcal{A}(\varpi))^2 \left((u_1(\mathcal{Q}_{in}))^2 \mathcal{V}_1(\varpi; \mathcal{Q}_{in}) - (u_1(c_1))^2\right.$$
$$\left. \times \mathcal{V}_1(\varpi; c_1)\right) - 2L_1(\varpi), \quad (13)$$

where $\ddot{f}(x) = d^2 f(x)/dx^2$ is the second-order derivative of f with respect to x, $c_{4,k} = (\pi\rho)^2 (\mathcal{B}_k)^{-1} (\mathcal{F}/K_0)^{\delta}$. (13) holds due to the monotonically decreasing behaviour of $\mathcal{V}_1(\varpi; x)\left((\mathcal{A}(\varpi) u_1(x))^2 + 2(1 + \mathcal{A}(\varpi) u_1(x))\right)$. To examine the behaviour of the EE when $\lambda \to 0$, we compute the limit of $\mathcal{P}(\omega)$ as follows:

$$\lim_{\varpi \to 0} \mathcal{P}(\varpi) = \lim_{\varpi \to 0} \frac{c_3 \upsilon_1}{\mathcal{BC}} \frac{\left(\mathcal{V}_1(\varpi; Q_{in}) - \mathcal{V}_1(\varpi; c_1)\right)}{\mathcal{A}(\varpi)} + c_3 \upsilon_4$$
$$= c_3 \upsilon_4 + \left(c_3 \upsilon_1 / (\mathcal{BC})\right)\left(u_1(c_1) - u_1(Q_{in})\right). \quad (14)$$

Finally, by substituting (14) into (11), we obtain $\mathcal{E}(\varpi \to 0)$.

Appendix III
Proof of Proposition 2

In this section, we prove the pseudo-concavity of the EE with respect to the transmit power, P_{tx}. By examining the numerator of the EE in (5) it follows that:

$$\mathrm{Num}\left(P_{\mathrm{tx}} = \varpi\right) = \sum_{k=7}^{12} \mathcal{G}_k \mathcal{P}_k(\varpi), \quad (15)$$

where $\mathcal{G}_k = \rho \lambda_k k N_{\mathrm{pac},k}$; from (15), it can be concluded that in order to identify the behaviour of $\mathrm{Num}(\varpi)$, we need to examine the trend of $\mathcal{P}_k(\varpi)$ that is summed multiple times over an arbitrary region. It should be noted that since the $\mathcal{P}_k(\varpi)$ summed over all regions, is identical in every region the subscript k, can be dropped for simplicity. Hence, the problem reduces to examining the trend of $\mathcal{P}_k(\varpi)$. The first and second-order derivatives of $\mathcal{P}_k(\varpi)$ are given by:

$$\dot{\mathcal{P}}(\varpi) = -\delta(\mathcal{D}(\varpi))^{-\delta-1}\left(\dot{\mathcal{D}}(\varpi)\right) c_3$$
$$\times \left[\mathcal{V}_1(\mathcal{D}(\varpi))\upsilon_6 + \exp\left(-\mathcal{A}\right)\upsilon_7\right] \geq 0$$
$$\ddot{\mathcal{P}}(\varpi) = -\delta(\mathcal{D}(\varpi))^{-\delta-2}\left(\dot{\mathcal{D}}(\varpi)\right)^2 c_3 \Big[\exp\left(-\mathcal{A} u_1(\mathcal{D}(\varpi))\right)\upsilon_6$$
$$\times \Big((1-\delta) + \delta\mathcal{ABC}(\mathcal{D}(\varpi))^{-\delta}\Big) + (1-\delta)\exp\left(-\mathcal{A}\right)\upsilon_7\Big] < 0, \quad (16)$$

where $\dot{\mathcal{D}}(\varpi) = -\left(\gamma_{\mathrm{D}}\sigma^2\right)/(\varpi)^2$, $\upsilon_6 = \mathbf{1}\left(\mathcal{Q}_{in} - \mathcal{D}\right)\mathbf{1}\left(\mathcal{D} - \gamma_I \mathcal{Q}_{out}\right)$ and $\upsilon_7 = \mathbf{1}\left(\mathcal{D} - \mathcal{Q}_{out}\right)\mathbf{1}\left(\min\left\{\gamma_I \mathcal{Q}_{out}, \mathcal{Q}_{in}\right\} - \mathcal{D}\right)$, $\left(\ddot{\mathcal{D}}(\omega)\right) = 2\left(\gamma_{\mathrm{D}}\sigma^2\right)/\omega^3 > 0$.

From (16), is demonstrated that $\mathcal{P}(\varpi)$ is concave function with respect to the transmit power. Moreover, from (5) it can be concluded that the denominator of the EE is an affine function with respect to the transmit power. Hence, the EE is a pseudo-concave function with respect to the transmit power [11, Proposition 2.9]. Let us denote $c_6 = \sum_{k=7}^{12} \rho\lambda_k T_{S_{3,k}}$ and $c_7 = \sum_{k=7}^{12} \left(\rho\lambda_k E_{\mathrm{cir},k} + (1-\rho)\lambda_k E_{\mathrm{sl},k}\right)$ then $P_{\mathrm{tx}}^* = VI_{\mathrm{tx}}^*$ is the root of the following non-linear equation.

$$\dot{\mathcal{E}}(P_{\mathrm{tx}}^*) = 0 \Leftrightarrow (P_{\mathrm{tx}}^* c_6 + c_7)\left(\sum_{k=7}^{12} \mathcal{G}_k \dot{\mathcal{P}}_k(P_{\mathrm{tx}}^*)\right) - c_6\left(\sum_{k=7}^{12} \mathcal{G}_k \mathcal{P}_k(P_{\mathrm{tx}}^*)\right) = 0, \quad (17)$$

P_{tx}^* is then a global maximum of the EE thanks to the property of pseudo-concave functions [12, Theorem 21.16] and can be straightforwardly computed with the help of software such as Matlab and Mathematica. QED.

References

[1] F. Tariq *et al.*, "A Speculative Study on 6G," *IEEE Wireless Commun.*, vol. 27, no. 4, pp. 118-125, August 2020.

[2] U. Raza *et al.*, "Low Power Wide Area Networks: An Overview," *IEEE Commun. Surveys Tuts.*, vol. 19, no. 2, pp. 855-873, 2017.

[3] J. P. S. Sundaram *et al.*, "A Survey on LoRa Networking: Research Problems, Current Solutions, and Open Issues," *IEEE Commun. Surveys Tuts.*, vol. 22, no. 1, pp. 371-388, First quarter 2020.

[4] C. Goursaud *et al.*, "Dedicated networks for IoT : PHY / MAC state of the art and challenges", *EAI Trans. IoT* , vol. 1, no. 1, 2015.

[5] O. Georgiou *et al.*, "Low Power Wide Area Network Analysis: Can LoRa Scale?", *IEEE Wireless Commun. Lett.*, vol. 6, no. 2, April 2017.

[6] L.-T. Tu *et al.*, "A New Closed-Form Expression of the Coverage Probability for Different QoS in LoRa Networks", in *Proc. IEEE ICC2020*, Dublin, Ireland.

[7] T. T. Lam *et al.*, "On the Energy Efficiency of Heterogeneous Cellular Networks With Renewable Energy Sources—A Stochastic Geometry Framework," *IEEE Trans. Wireless Commun.*, vol. 19, no. 10, Oct. 2020.

[8] M. Di Renzo *et al.*, "System-Level Modeling and Optimization of the Energy Efficiency in Cellular Networks – A Stochastic Geometry Framework", *IEEE Trans. Wireless Commun.*, vol. 17, no. 4, Apr. 2018.

[9] L. Casals *et al.*, "Modeling the Energy Performance of LoRaWAN," *Sensors* 2017, 17, 2364.

[10] IEEE 802.16p-11/0014, *IEEE 802.16p Machine to Machine (M2M) Evaluation Methodology Document (EMD)*. [Online]. Available: http://ieee802.org/16/m2m/index.html

[11] A. Zappone *et al.*, "Energy Efficiency in Wireless Networks via Fractional Programming Theory", *Foundations and Trends in Commun. and Inf. Theory*, vol. 11, no. 3-4, 2014, pp. 185-396.

[12] C. P. Simon *et al.*, "Mathematics for economists", W. W. Norton, 1994.